Decoupling CME Temporal Properties from Solar Cycle Effects.

Yakub Olufadi[1], Nada Al-Haddad[1], Noé Lugaz[1], Bin Zhuang[1], Charlie Farrugia[1], Christian Moestl[2]

[1]University of New Hampshire [2]Austrian Space Weather Office

1. Introduction

Previously, we have studied the effect of the solar cycle (SC) on typical CME properties (Olufadi et al., 2025) in prep & (Regnault et al., 2021); therein, it was established that virtually all CME features vary with the observed variation in SC activity according to Figure [1]. We are currently conducting a more detailed analysis of the CME profile to differentiate the effects of the solar cycle from the inherent characteristics of the CMEs. For this study, we selected events near 1 AU from over 1600 CME timestamps stored in the HELIO4CAST catalog (Möstl, et al., 2017).

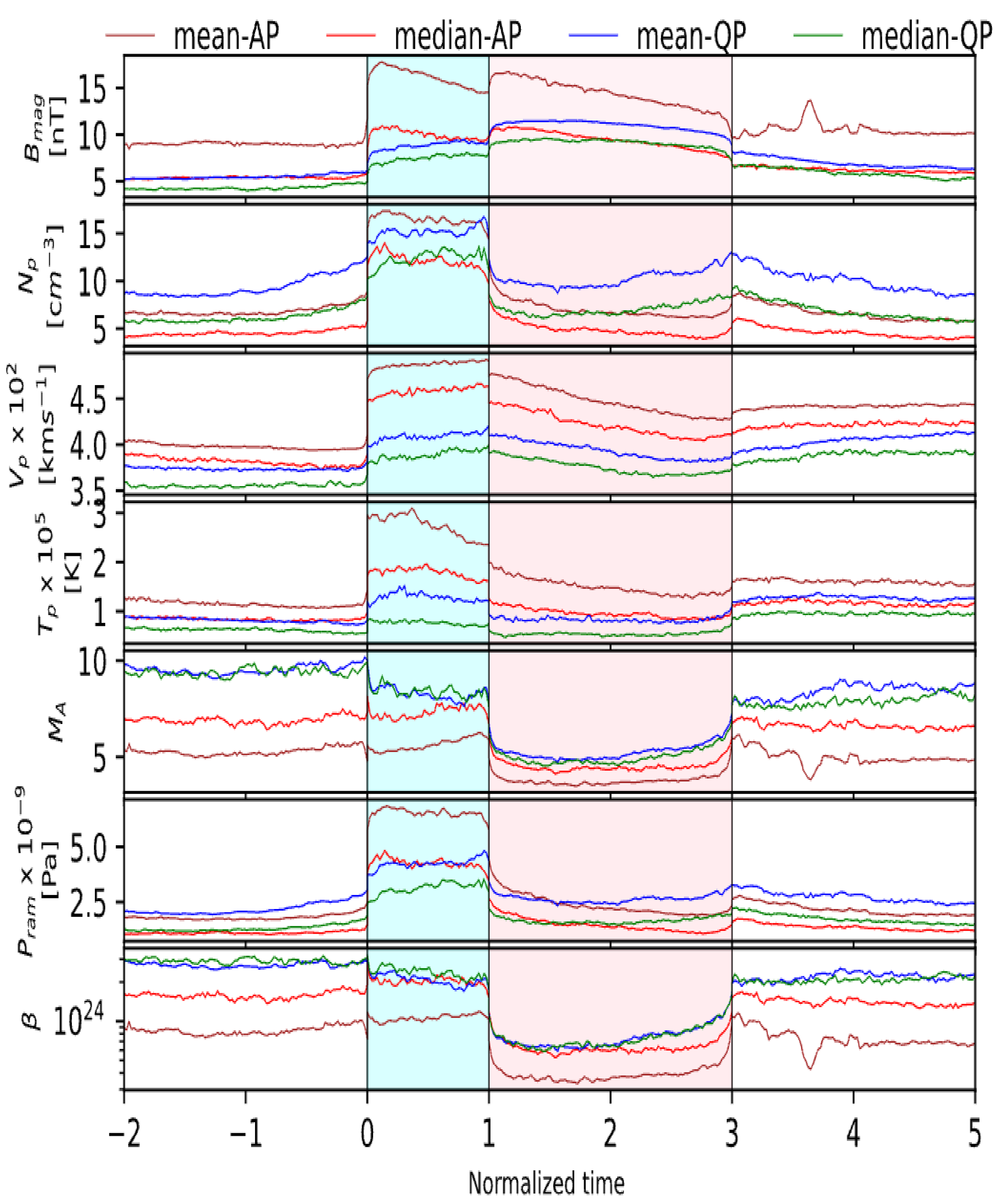

Figure 1. The combined SEA plot of AP and QP events.

2. Method: SEA for Matching AP & QP Events

Active Phase (AP) and Quiet Phase (QP) are matched to the same frequency to prevent data fluctuation.

SEA Result: Overall, both B_{mag} and V_p are enhanced for AP events, indicating a stronger, more compressed sheath consistent with fast CME dynamics, while the ME region reveals a peculiar B_{mag}–V_p relationship.

The enhanced B_{mag} and V_p in the ME region indicate that CMEs retain their core magnetic and dynamic properties (coherent flux rope structure), while the drop in B_{mag} and V_p in the sheath reflects a disturbed, turbulent, and compressed solar wind environment.

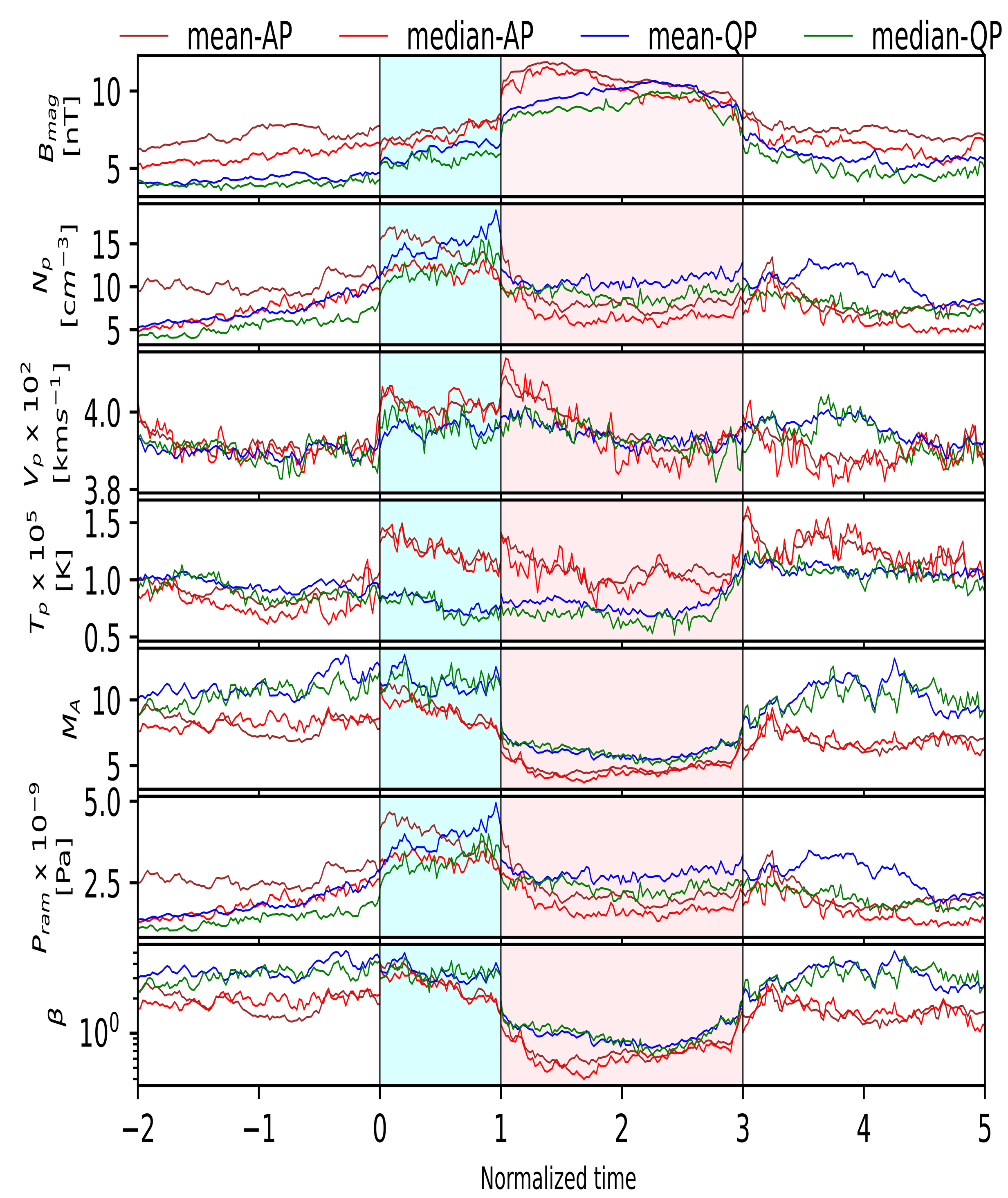

Figure 2. SEA for matching AP and QP events.

3. Heliocentric Distance Dependence

Variational study of CME feature as a function of heliocentric distance.

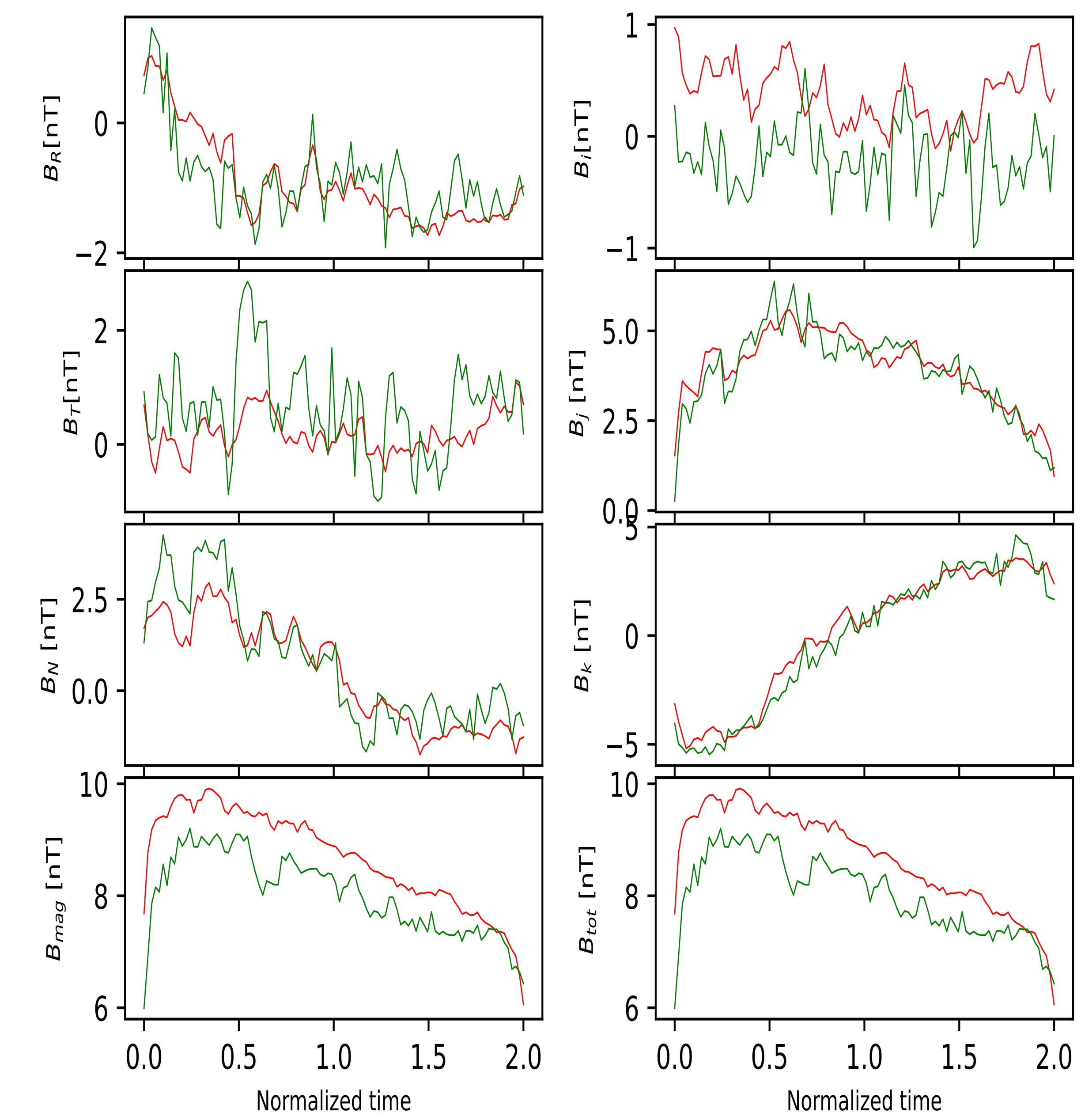

Figure 3. Sample SEA for B_{field} components: RTN vs MVA plot of AP and QP events.

We also study the variation in axial and poloidal MVA magnetic field components as a function of heliocentric distance for all CME bins in this study.

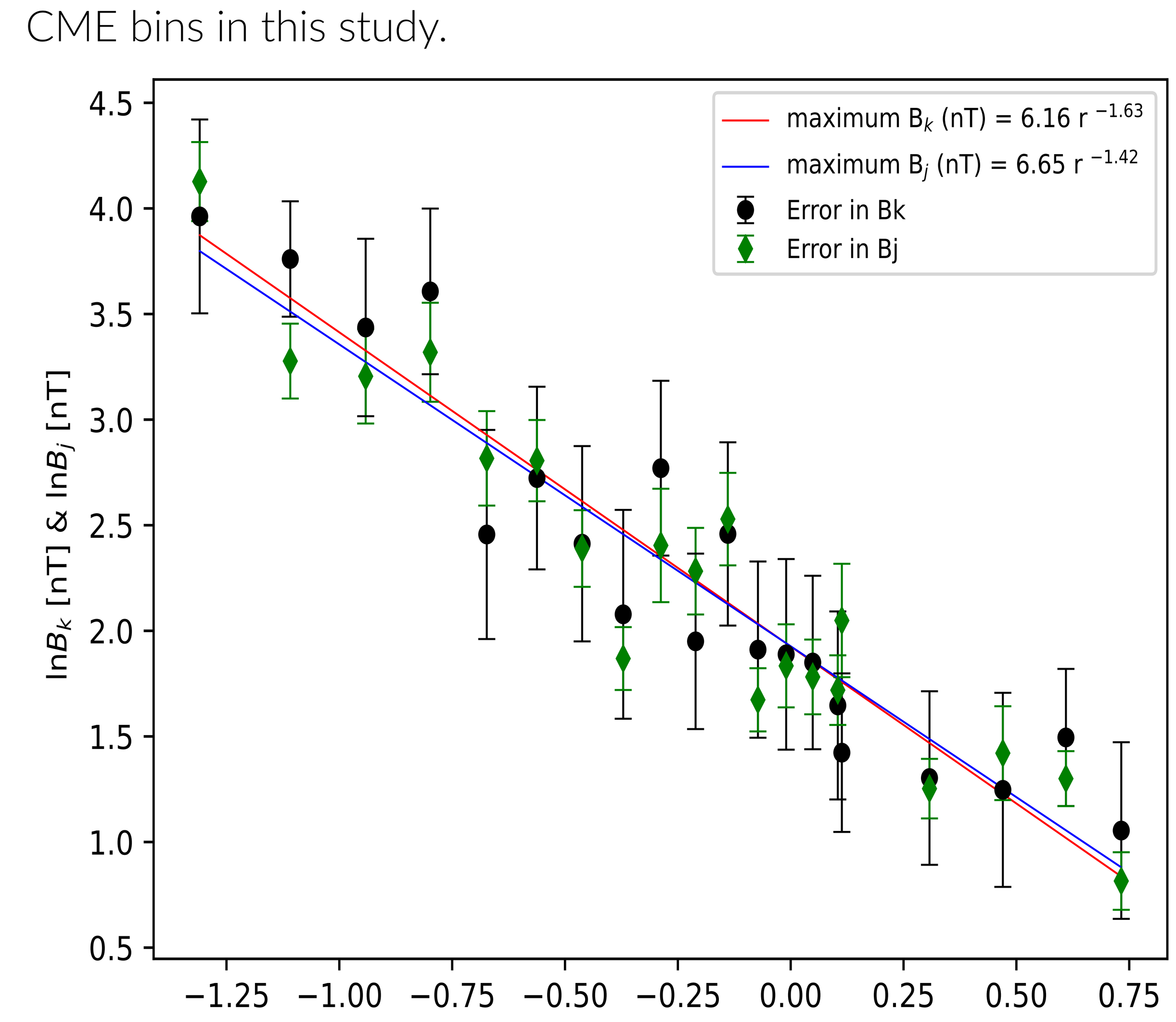

Figure 4. The plot of ln max. B_k ln max. B_j Vs. helio-dist. [ln mid-bin]

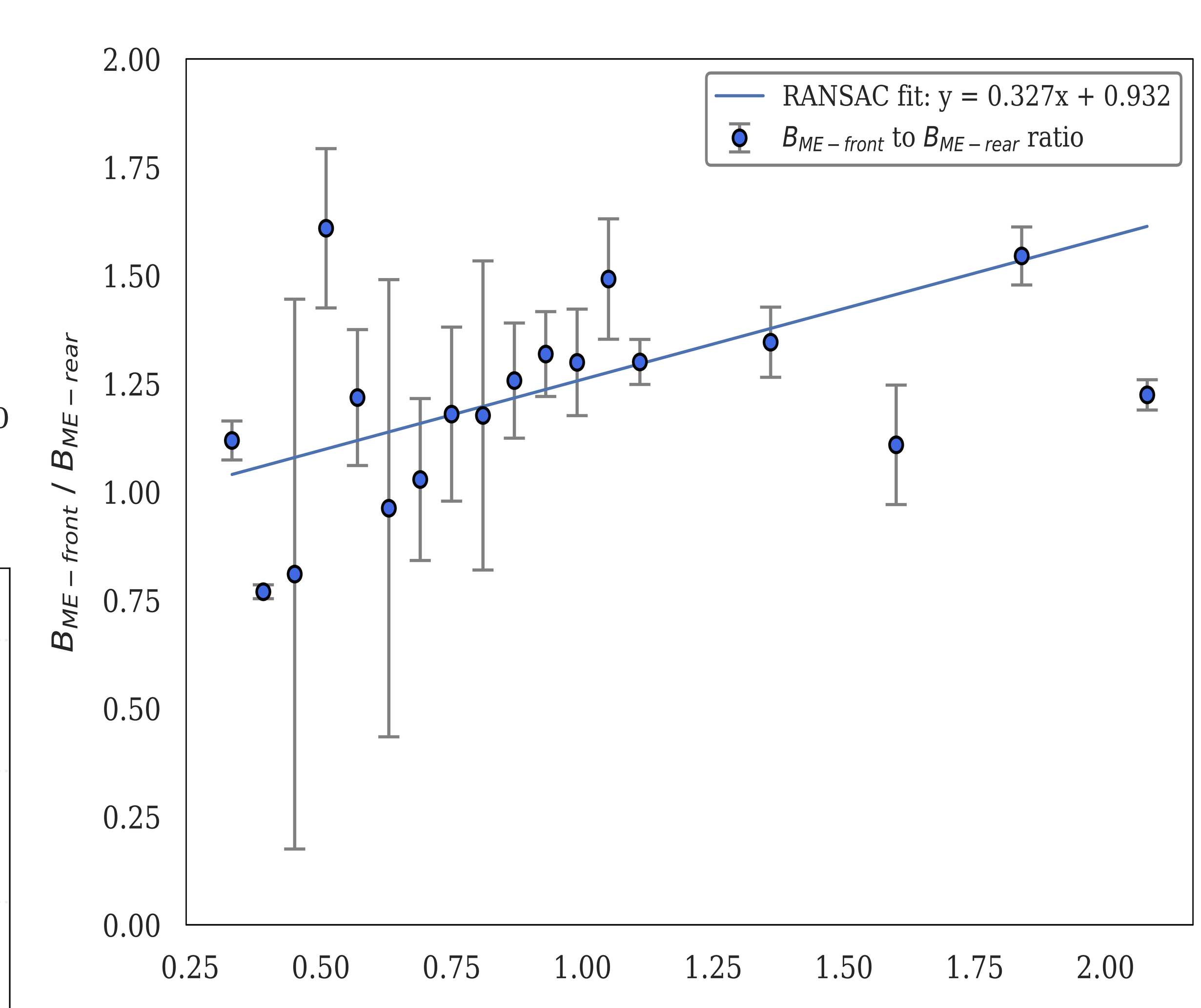

Figure 5. The ratio of average B_{ME} (front-rear) vs. helio-dist.

4. Sheath-ME Relation

The result of Pearson (C_p) and Spearman (C_s) correlation study between V_{ME} & V_{sheath} for nearly of all the CME bins is shown below. Our correlation coefficients agrees with (Janvier et al., 2019):(C$_s$ = 0.77, C$_p$ = 0.80)

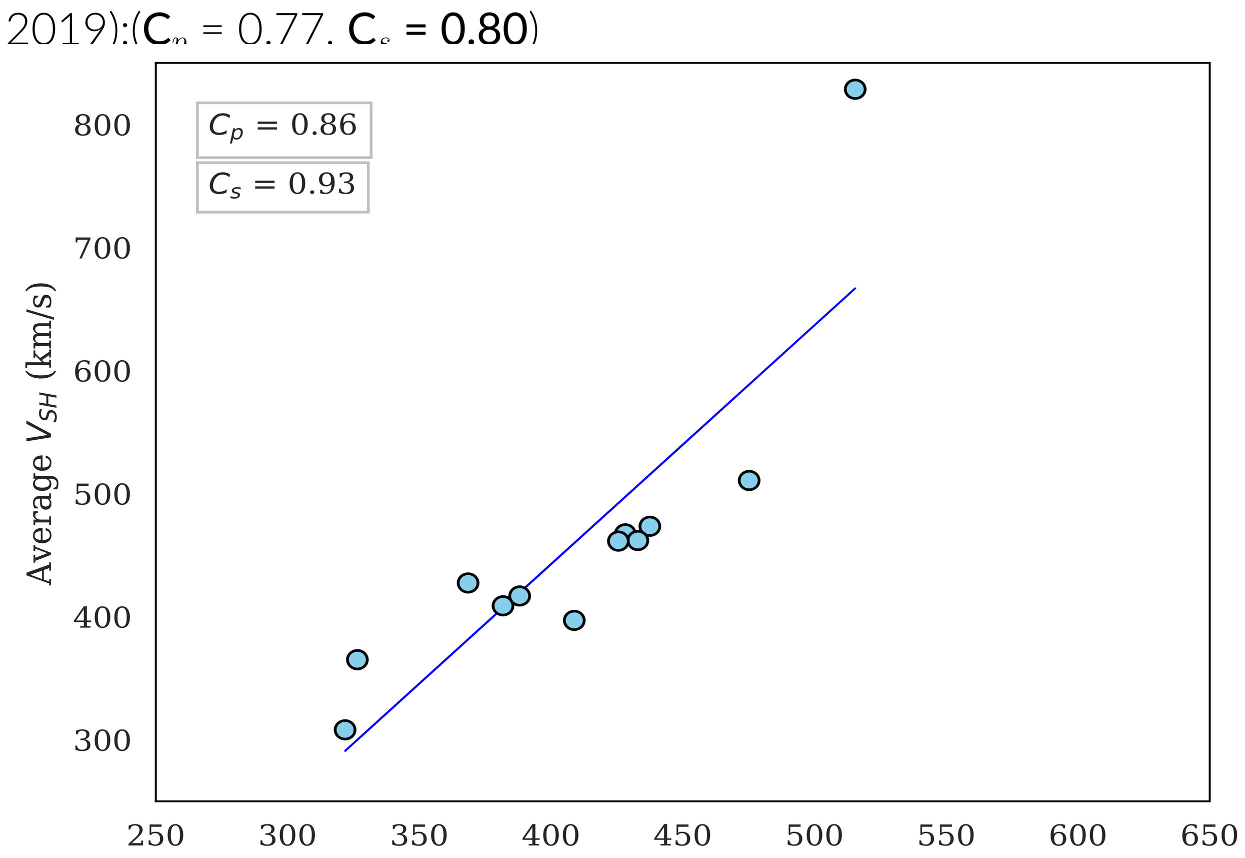

Figure 6. Correlation between V_{ME} and V_{SH}.

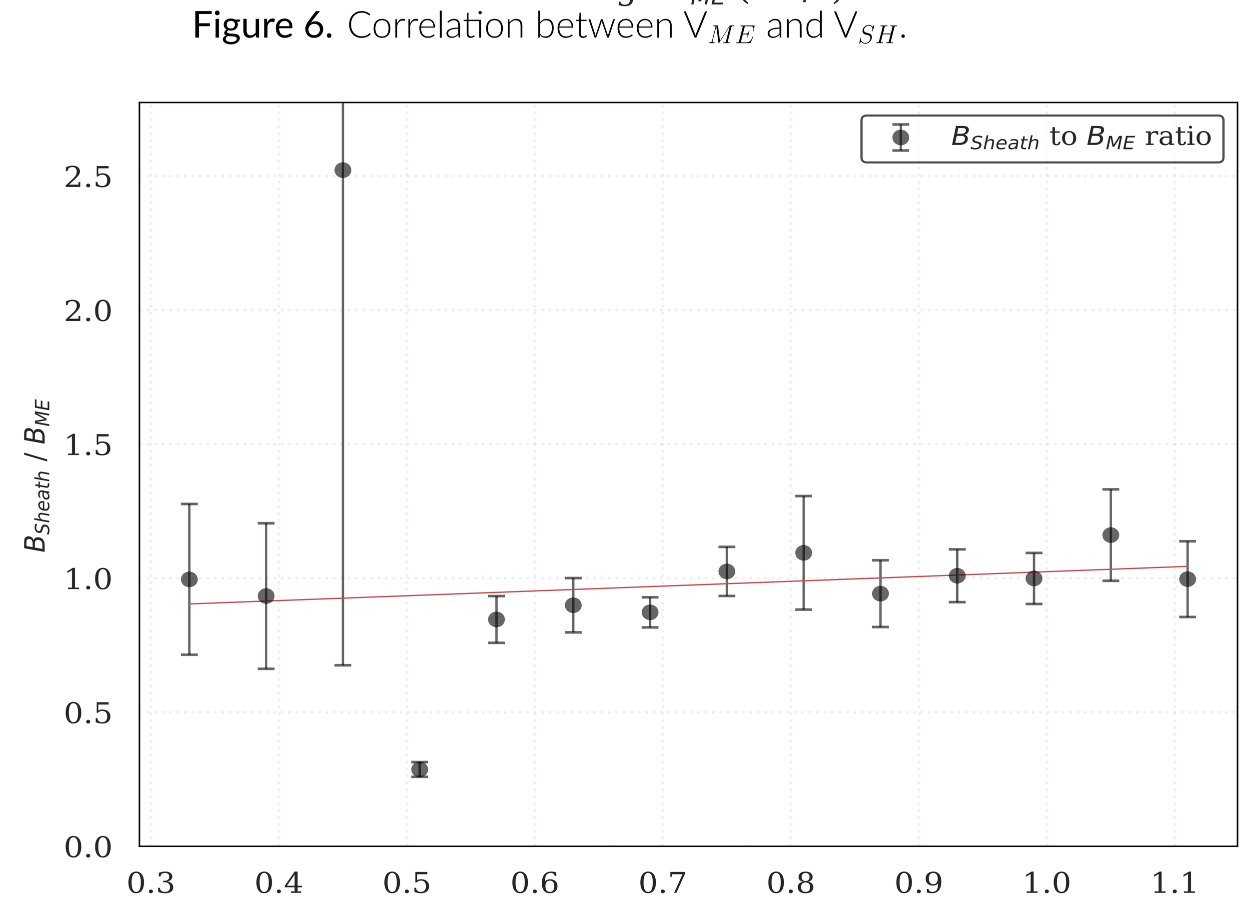

Figure 7. Sheath-ME ratio relative to heliocentric distance.

5. Result Summary

- Generally, in the presence of shocks—more likely during active solar phases, the sheath region shows strong B_{mag} and V_p enhancements due to solar wind compression. Without shocks, a typically sheath enhancements are weaker, but in all cases, the ME region maintains higher B_{mag} and V_p due to its intrinsic flux rope structure. The reflect largely inherent temporal feature of a typical CME independent of solar cycle
- The consistent structural features observed at the front and rear of the ME region in both B_{mag} and V_p profiles (rapid boundaries decline and steady velocity decline) also indicate an inherent properties of CME dynamics, particularly due to expansion and magnetic coherence.Also, this similarity suggests that the observed behavior could not have been governed by SC phase, but probably reflects the core physical structure of CMEs themselves.
- Similar decrease rates of B_j and B_k in Figure [4] suggest that the coronal mass ejection (CME) expands at comparable rates along both its radial and axial directions, indicating a uniform expansion behavior in these dimensions.
- Figure [5] Most values are greater than 1, indicating that the magnetic field strength at the front of the ME is generally stronger than at the rear and that the strengths age as the CME propagates.
- The strong correlation between V_{sheath} & V_{ME} in Figure [6] emphasizes that the sheath is being driven by the ME which further indicates that sheath dynamics are primarily governed by CME propagation speed.

6. References

Janvier, M., Winslow, R. M., Good, S., et al. 2019, Journal of Geophysical Research (Space Physics), 124, 812, doi: 10.1029/2018JA025949

Möstl., C., Isavnin., A., Boakes., P. D., et al. 2017, Space Weather, 15, 955

Olufadi, Y., Al-Haddad, N., Lugaz, N., et al. 2025, arXiv e-prints. https://arxiv.org/abs/2506.xxxxx

Regnault, F., Dasso, S., Auchere, F., et al. 2021, in 43rd COSPAR Scientific Assembly. Held 28 January - 4 February, Vol. 43, 1017

7. Acknowledgement

This research is being supported by NSF grant (AGS1954983), and NASA grants (80NSSC21K0463 & 80NSSC22K0349).

ybo1000@unh.edu